ELSEVIER

Surface Science 398 (1998) 184–194

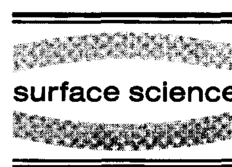

Surface electronic structure of pure and oxidized non-epitaxial Mg_2Si layers on Si(111)

M. Brause, B. Braun, D. Ochs, W. Maus-Friedrichs *, V. Kempter

Physikalisches Institut der Technischen Universität Clausthal, Leibnizstraße 4, 38678 Clausthal-Zellerfeld, Germany

Received 7 May 1997; accepted for publication 2 October 1997

Abstract

Non-epitaxial magnesium silicide (Mg_2Si) films of 100 Å thickness were grown on Si(111). The formation of Mg_2Si is identified by characteristic shifts of the Mg 2p and Si 2p peaks in X-ray photoelectron spectroscopy (XPS). Information on the electronic structure of this surface is obtained by metastable impact electron spectroscopy (MIES). The surface density of states obtained with MIES is dominated by strong emission below the Fermi level (E_F) displaying a characteristic double peak structure. The oxidation of these silicide surfaces is performed at room temperature. The electronic structure of these surfaces is investigated with MIES, UPS (HeI) and XPS. From the comparison with oxidized Mg films it is concluded, that the surface is terminated by an insulating MgO layer. Subsurface oxidation of the silicide does not take place. Furthermore, no formation of silicon oxides is observed. © 1998 Elsevier Science B.V.

Keywords: Electronic structure; Insulating film; Magnesium silicide; Metastable impact electron spectroscopy; Oxidation; Photoelectron spectroscopy

1. Introduction

Silicides have received increasing interest during the last decade. This interest concerns both technological and fundamental aspects of silicides. A fundamental review can be found in Ref. [1], a review focusing on transition metal silicides in Ref. [2]. Briefly some of the main aspects will be discussed.

Silicon–metal contacts are accompanied by the formation of Schottky barriers. Using transition metals the Schottky barrier heights vary between 0.4 and 0.93 eV [1]. Due to the fact that the silicide interface layer can be rather small the investigation of the microscopic and electric properties of Schottky barriers has become possible. Silicides have been produced from thin interface layers with a thickness of some Ångstrom up to thicknesses of some hundred microns. Depending on the composition and on the temperature silicides with different stoichiometries were found to be stable. For example nickel silicide can be formed as Ni_3Si, Ni_5Si_2, Ni_2Si, Ni_3Si_2, NiSi and $NiSi_2$; the latter is the most stable one. Many silicides are found to be conductors like $NiSi_2$, $CoSi_2$ and most of the other transition metal silicides. In contrast, $OsSi_2$, $CrSi_2$ and Mg_2Si are semiconductors. $FeSi_2$ in its tetragonal lattice structure is also

* Corresponding author. Fax: (+49) 5323 723600: e-mail: wmf@physik.tu-clausthal.de

0039-6028/98/$19.00 © 1998 Elsevier Science B.V. All rights reserved.
PII S0039-6028(97)00774-7

conducting, but this configuration is only stable for temperatures beyond 967°C. Below this temperature the lattice is orthorhombic and also semiconducting [3]. The conducting silicides are low work function metals and may be applied as photocathodes. The semiconducting silicides possesses small band gaps and may find application in optoelectronic devices.

Magnesium silicides are different compared to most other silicides because the only possible stoichiometry is Mg_2Si. It has a cubic CaF_2 structure with a lattice constant of 6.39 Å [4]. Mg_2Si is a semiconductor with a direct band gap of 2.17 eV and an indirect band gap of 0.6 eV [5]. In contrast to transition metal and noble metal silicides which display a metallic bonding, Mg_2Si bonds covalently with ionic contributions [6]. Most of the investigations so far published dealing with the Mg–Si interface are concerned with the geometric structure and the character of the binding in the submonolayer range for Si(111) substrates [7–9] and Si(100) substrates [10]; epitaxial growth on Si(111) was observed for submonolayers and thin layers on Si(111).

The oxidation of silicides is of technological interest for microelectronic devices. It may turn out, that oxidized silicide surfaces are useful as insulating layers on semiconducting devices. Additionally, the interaction of new materials with oxygen and other gases may be of fundamental interest for the understanding of chemisorption processes.

The results for the oxidation of noble metal silicides show that the noble metal serves as catalyst for the silicon oxidation [11]. The free energy for SiO_x formation is much higher than the one for noble metal oxide. Therefore no noble metal oxidation occurs. For metal rich silicides like Pt_2Si, SiO_2 formation is found while for metal poor silicides like $PtSi_2$ silicon suboxides like $Si(SiO_3)$ and $Si(Si_3O)$ are observed [11].

For the transition metals, whose free energy for oxide formation is higher than that for noble metal oxidation, mixtures of SiO_x and metal oxide complexes can be found depending on the material and silicide composition. The oxidation of the metal rich silicide Ni_2Si for example produces nickel oxides to some extent while the oxidation of the metal poor silicide $NiSi_2$ produces SiO_x top layers without any metal oxide [11]. The oxidation of $TiSi_2$ in contrast produces both TiO_2 and SiO_2 to a comparable amount [12].

A study of the electronic properties of magnesium silicide formation on Si(111) and the oxidation of magnesium silicide films applying ultraviolet photoelectron spectroscopy (UPS) using HeI photons and metastable impact electron spectroscopy (MIES) using $He^*(2^3S)$ probe atoms is reported. MIES and UPS results are discussed in combination with X-ray photoelectron spectroscopy (XPS) results which show significant peak shifts of the Mg and Si derived peaks during silicide formation and oxidation. Additionally, low energy electron diffraction (LEED) is applied for the study of the silicide layer geometry.

UPS and MIES are surface sensitive techniques. UPS shows in principle a mixture of the surface density of states (SDOS) and the bulk density of states (BDOS) with the restriction, that the final density of states has to be taken into account. MIES in contrast gives information only from the outermost layer which displays the density of states projected to the outermost orbitals [13]; final state effects are much less important. Applying MIES, metastable $He^*(2^3S)$ atoms approach to the surface with thermal kinetic energy, which leads to different interaction processes emitting electrons:

(1) As soon as a surface wave function overlaps with the He 1s orbital an Auger De-excitation (AD) process occurs when the surface work function is below 3.5 eV [14]. Hereby a surface electron fills the He 1s vacancy thus emitting the electron in the He 2s orbital carrying the excess energy. The kinetic energy distribution of these electrons mirrors the density of states projected to the impinging He*. It is called the projected DOS (PDOS).

(2) In cases where the surface work function exceeds 3.5 eV the impinging He* is resonantly ionized and an Auger Capture (AC) process takes place where the electron energy distribution is formed by a self convolution of the PDOS. It will be shown in Section 3, that this process is not relevant for the purpose of this paper and will therefore not be discussed any further.

(3) For work functions below ca 2.2 eV an additional process becomes important [15]. Hereby a surface electron is resonantly transferred into the He 2s orbital thus producing a negative excited He^{-*} $1s2s^2$ ion in front of the surface. This ion decays via a fast autodetachment process into ground state producing an atomic-like line near a kinetic energy of 19 eV.

On insulating surfaces, which are formed during the oxidation of Mg_2Si, only the AD process is possible. This follows from the absence of unoccupied surface orbitals being in resonance with the He 2s orbitals. Further details of the $He^*(2^3S)$–surface interaction for AD and AC processes can be found in Ref. [14]; details for the autodetachment process may be found in Ref. [15].

2. Experimental techniques

The apparatus has been described in detail previously [16,17]. Only a brief review will therefore be given.

The apparatus is equipped with a cold-cathode gas discharge source for the production of metastable $He^*(2^3S/2^1S)$ ($E^* = 19.8/20.6$ eV) atoms with thermal kinetic energies and HeI photons ($E^* = 21.2$ eV) for UPS. The triplet to singlet ratio amounts to 7:1 [13]. $He^*(2^1S)$ atoms are known to be converted into $He^*(2^3S)$ atoms in front of metallic and semiconducting surfaces very efficiently [18–20]. Therefore almost no contributions induced by $He^*(2^1S)$ atoms are found in the spectra. Metastable and photon contributions within the beam are separated by means of a time of flight technique combined with a twin counter system allowing the simultaneous measurement of MIES and UPS spectra. The angle of incidence of the probe beam is 45°; electrons emitted in the direction normal to the surface are analysed. The simultaneous collection of a MIES/UPS spectrum requires 2 min. The apparatus is further equipped with a commercial X-ray source (Specs model 865) for XPS. MIES, UPS and XPS measurements are performed using a hemispherical analyser (VSW HA100) with an energy resolution of 250 meV for MIES/UPS and of 0.5 eV for XPS. All spectra are displayed as a function of the binding energy. Additionally the apparatus is equipped with the equipment for low energy electron diffraction (LEED) (Physical Electronics Industries 11-020) and Auger electron spectroscopy (AES) (Physical Electronics Industries 11-500A).

MIES and UPS experiments are performed biasing the target by 50 eV, which has been shown to have almost no influence on the spectral features. The Fermi energy (E_F), which corresponds to zero binding energy ($E_B = 0$) is determined from the spectra by electrons emitted from metallic substrates with the maximum kinetic energies. The MIES/UPS source offers ca 10^9 He* and ca 10^{10} HeI photons per s mm^{-2} on the target; the ejected electrons are detected by the hemispherical analyser.

Si(111) samples were prepared from As doped Si wafers with a resistivity of ca 0.005 Ωcm. The Si surfaces were prepared by warming up to ca 800 K for 10 min followed by four to five flash cycles at a temperature of ca 1600 K for 5 s, respectively. Afterwards the surface temperature is reduced to room temperature slowly in 10 min. Details of the preparation have been published previously [21]. Surface cleanness was checked using XPS, MIES and LEED. Due to the fact that Mg_2Si has a high temperature stability Si targets cannot be cleaned by a heating procedure after silicide formation has taken place. Therefore a new Si(111) target was introduced for every measurement cycle.

Mg_2Si layers are produced by evaporating Mg from a commercial Knudsen cell on the Si(111) surfaces held at a substrate temperature of 570 K for 10 min. The Mg evaporation is done at a cell temperature of 600 K thus evaporating 4 monolayers (ML) of Mg min^{-1}. The thickness of the Mg_2Si layer on the Si surfaces is estimated on the basis of the ratio of Si 2p and Mg 2p peaks obtained with XPS.

Oxygen is offered using a ultra-high vacuum (UHV) leak valve with partial pressures between 2×10^{-9} and 5×10^{-8} Torr. The pressure is measured using a standard ion gauge. To observe the changes of the electronic structure during the oxidation process oxygen is offered to a small rate

continuously while MIES and UPS spectra are collected.

The base pressure of the apparatus amounts to 7×10^{-11} Torr; during evaporation of Mg the pressure increases to 3×10^{-10} Torr.

All spectra shown below are displayed as a function of the binding energy (E_B) referring to the target Fermi level.

3. Results and discussion

3.1. Mg_2Si formation on Si(111)

The thickness of the produced Mg_2Si layers amounts to (100 ± 10)Å in all cases, which has been estimated from XPS measurements not shown here. LEED investigations showed no ordered structure for the produced Mg_2Si films. It has been found previously, that non-epitaxial Mg_2Si films grown on Si(100) at room temperature have a limited thickness of 2 ML [10] corresponding to ca 13 Å. Applying the template procedure (repeated adsorption of 10–30 ML of Mg and subsequent heating) at a substrate temperature of 570 K epitaxial Mg_2Si layers on Si(111) are limited to a similar thickness [5]. In both cases XPS spectra show contributions from pure Si and Si bound in Mg_2Si simultaneously, which is not the case in our XPS measurements. At room temperature the Mg_2Si top-layer decreases the diffusion probability for Mg and therefore the film thickness is limited [10]. Using the template procedure on Si(111) the diffusion probability for additional Mg is increased after formation of the epitaxial Mg_2Si layer. But in contrast, the sticking coefficient for Mg on the Mg_2Si surface is reduced so that also in this case no further silicide formation occurs. Offering Mg to the Si(111) surface at elevated temperatures (570 K in this case) bypasses both problems [10]. On the basis of this consideration and based on the LEED results it is concluded that the thick layers produced by this procedure are non-epitaxial.

Fig. 1a shows the Si 2p XPS spectra for the clean Si(111) surface and the thick Mg_2Si layer; Fig. 1b shows the corresponding Mg 2p XPS

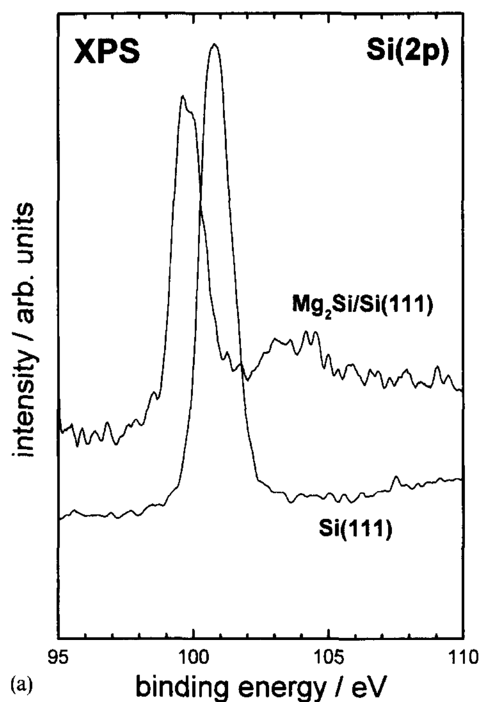

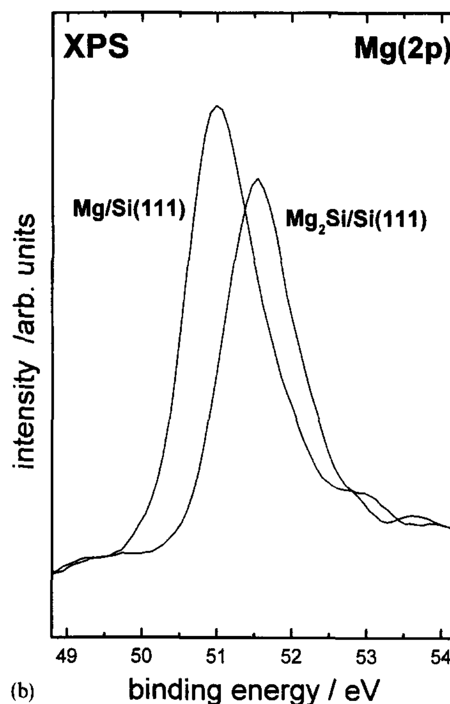

Fig. 1. XPS spectra of (a) the pure Si(111) and a thick (100 Å) Mg_2Si layer for the Si 2p peak and (b) a pure Mg film and the same Mg_2Si layer for the Mg 2p peak.

spectra for a pure Mg film and the thick Mg_2Si layer. Si 2p is found to shift by −1.1 eV from a binding energy E_B of 100.8 to 99.7 eV during the Mg exposure. In addition, a small peak at E_B = 104 eV appears during the silicide formation which is one of the satellite peaks belonging to the Mg 2s emission at 91.4 eV (not shown here). The Mg 2p peak in contrast shifts by +0.6 eV to higher binding energies compared with pure Mg films [13] from E_B = 51.0 to 51.6 eV. These core level shifts have also been observed for epitaxial Mg_2Si layers on Si(111) [5] and non-epitaxial Mg_2Si layers on Si(100) [10] and were attributed to the formation of Mg_2Si, which is the only possible magnesium silicide. Both peaks at 51.0 eV (Mg film) and 51.6 eV (silicide) can be fitted by Gaussian peaks of the same width. However it was not possible to fit the peak at 51.6 eV assuming contributions from a second peak at E_B = 51.0 eV (corresponding to unreacted Mg). This means, that within the accuracy of the measurements (below 5%) no contributions corresponding to unreacted Mg are present in the Mg_2Si layer. It is therefore concluded, that the thick non-epitaxial layers produced on Si(111) by the simple procedure applied here consist entirely of Mg_2Si.

Fig. 2 shows the MIES spectrum of the Mg_2Si surface corresponding to the top spectra of Fig. 1aFig. 1b. It is not "a priori" clear to what extent AC and AD processes contribute to the electron emission. Additional information clearing up this question can be obtained from the simulation of the MIES spectra on the basis of the numerical procedure developed by Niehaus and co-workers [22,23], which has already previously been applied for the interpretation of He*–surface interaction processes (see, for example, Refs [13,24,25]). Both AD and resonance ionization (RI) followed by AC are allowed for. Transition rates for the resonant and Auger processes which appear physically plausible on the basis of previous results were employed. The potentials describing the interaction of He*, He^+ and He^0 with the surface are estimated as described in Refs [22,23]. For the density of occupied states the results of Tejeda and Cardona shown in Fig. 2 are used [6]. The calculations are performed for the measured work function of 3.3 eV. For simplicity the small

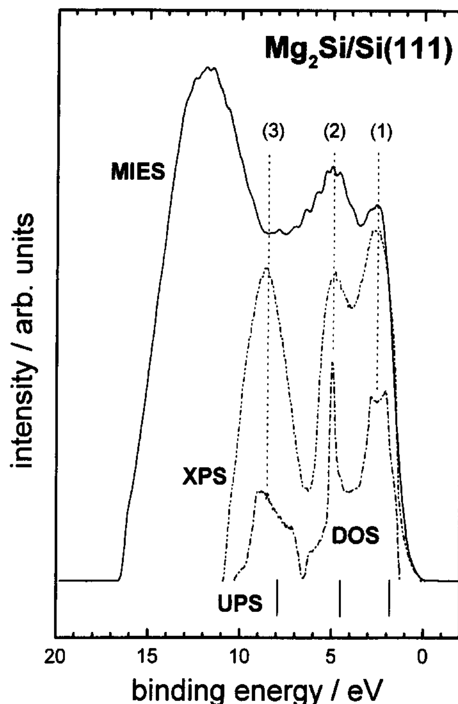

Fig. 2. MIES spectrum of a thick (100 Å) Mg_2Si layer compared with the calculated DOS and the valence band XPS spectrum of polycrystalline Mg_2Si (from Ref. [6]) and the UPS (108 eV) peak positions of expitaxial Mg_2Si on Si(111) (from Ref. [5]).

band gap of the semiconductor was neglected. Under these conditions, the MIES spectrum turns out to be entirely due to AD, because for a He* kinetic energy of 100 meV the He 2s never comes in resonance with unoccupied states at the surface thus inhibiting the RI process. Moreover, the simulated MIES spectra reproduce the density of states involved in the AD process. This supports the statement made in Section 1, that MIES determines directly the SDOS (for more details see Ref. [13]).

Additional to the MIES the theoretical DOS and the XPS results for polycrystalline Mg_2Si published by Tejeda and Cardona [6] and the positions of the UPS peaks obtained using 108 eV photons for an epitaxial Mg_2Si layer on Si(111) published by Wigren et al. [5] are included in Fig. 2. Apart from the emission from secondary electrons on the left side (below E_B = 10 eV) the MIES spectrum displays two peaks at: (1)

$E_B = 2.5$ eV; and (2) 5.0 eV, which are similar to the corresponding theoretical and experimental peaks (1) and (2) published by Tejeda and Cardona [6]. The peaks obtained by Wigren display the same relative distance, but are shifted to lower binding energies by ca 0.5 eV. It is well known, that the cross-section for photoionization of s-states strongly depends on the photon energy. For the photon energy of the HeI line (21.2 eV) the photoionization cross-section almost vanishes [26]. Therefore s-states are hardly detected and UPS shows almost no contributions from s-states, which has also been demonstrated for Mg layers [13] and adsorbed alkali atoms [27,28]. Additional UPS measurements (not shown here) on the Mg_2Si surface therefore required a measuring time of several hours. During this time an oxygen contamination from the residual gas occurred corresponding to ca 2 L (1 L $= 10^{-6}$ Torr·s^{-1}), which is very similar to the HeI UPS spectra published by Cardona et al. [29], who reported the same oxygen induced problem.

On the basis of their calculations for the polycrystalline Mg_2Si films Tejeda and Cardona [6] remarked, that the doublet peak structure below E_F (1) and (2), which is also found with MIES, arise from s–p-hybrid states, while the contributions in the range between $E_B = 4$ and 10 eV (3) arise from the ionization of p-like states. Following this it may be suggested, that the two peaks (1) and (2) below E_F correspond to these states. On the basis of the measurements it is not possible to determine the kind of bonding. Therefore this question will not be discussed further within this paper.

Using MIES no differences in the interaction mechanisms occur for s- and p-like surface orbitals. The slow impinging He* atom interacts with the very outermost tail of the surface wave function in a distance between 5 and 2 Å in front of the surface. The MIES spectrum in Fig. 2 shows, apart from the contribution of secondary electrons at low kinetic energies, only the two peaks (1) and (2). Alkali and earth alkali surfaces show a similar behaviour: the MIES spectra for these systems are also mostly dominated by s-states just below E_F. The fact that such a strong intensity is found below E_F indicates that the Mg 3s electrons remain mostly located at the Mg atom. This suggests in combination with the relatively small Mg 2p core level shift due to the silicide formation, that the bonding of the Mg_2Si layer is mostly covalent.

Peak (3) is not visible with MIES, although it may be hidden by the secondary emission below $E_B = 10$ eV to some extent. This absence is probably caused by the spatial distribution of the wave function: the impinging He* interacts predominantly with the charge density of states in this energy range with the largest spatial distribution normal to the surface. It must therefore be assumed that the charge density of states corresponding to peak (3) does not protrude wide enough into the vacuum to interact efficiently with the impinging He*.

3.2. Oxidation of Mg_2Si layers

Fig. 3 shows UPS spectra obtained during the oxidation of the Mg_2Si film. The oxygen exposure increases by 0.25 L per spectrum. The left onset of

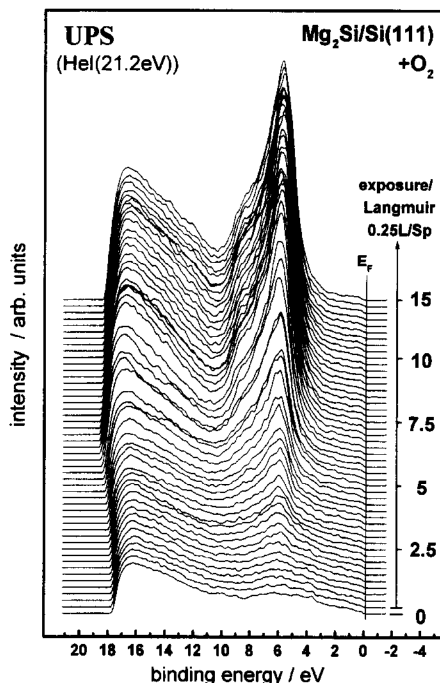

Fig. 3. UPS spectra of a Mg_2Si film (100 Å) during oxidation. The bottom spectrum displays the Mg_2Si layer; the oxygen exposure increases by 0.25 L per spectrum.

the spectra reflects the surface work function which decreases from 3.3 eV for zero exposure to 2.8 eV for an exposure of 15 L. At $E_B = 6$ eV a prominent structure develops with a shoulder at $E_B = 8.5$ eV. The structure saturates for oxygen exposures of 7.5 L. The contributions just below E_F decrease in intensity, but do not vanish completely. A similar structure, arising from the ionization of O 2p derived orbitals, is found during the oxidation of polycrystalline Mg and Mg films [13].

Fig. 4 shows the corresponding MIES spectra. Around $E_B = 6.0$ eV again a structure develops, which is markedly broader than in UPS. In contrast to the UPS measurements, the shoulder at $E_B = 8.5$ eV is much less pronounced. For MgO surfaces also only one similar structure was observed with MIES which corresponds to the ionization of O 2p derived orbitals. The difference of this structure obtained with MIES and UPS follows from the orientation of the O 2p orbitals in the top layer: the O $2p_z$ orbital, which is oriented perpendicular to the surface, produces the structure at $E_B = 6.0$ eV. The O $2p_z$ orbitals exhibit the largest spatial distribution perpendicular to the surface and therefore the impinging He* interacts predominantly with these orbitals. The O $2p_{x,y}$ orbitals oriented parallel are responsible for the shoulder at $E_B = 8.5$ eV [13]. For exposures beyond 7.5 L an insulator band gap develops below E_F. The maximum energy of the valence band is found at $E_B = 3.5$ eV, which is similar to the value for MgO surfaces [13].

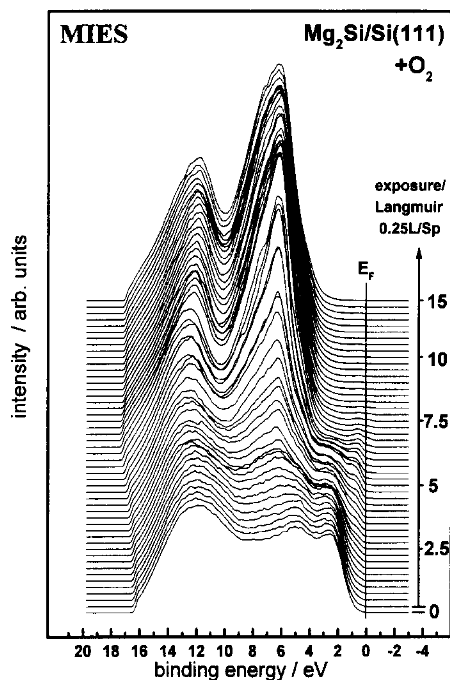

Fig. 4. MIES spectra of a Mg_2Si film (100 Å) during oxidation. The bottom spectrum displays the Mg_2Si layer; the oxygen exposure increases by 0.25 L per spectrum.

The MIES spectra for the oxidized surface show additional intensity around $E_B = 12$ eV. Similar features have also been observed for oxidized Mg layers [13,30]. Briefly, they correspond to the formation of a molecular species containing oxygen, most probably a CO_3^{2-} complex, formed at surface corners and kinks. These complexes can be removed easily by mild heating and are not of importance for the aim of this paper.

In the oxygen exposure range between 3 and 7 L an additional distinct feature just below E_F appears in the MIES spectra. This peak is most probably due to autodetachment of He^{-*} ions produced in front of the surface by the resonant transfer of a surface electron into the He 2s orbital. The probability for this resonant transfer increases strongly with decreasing work function, but decreases rapidly with the decreasing number of occupied states just below E_F due to the forthgoing oxidation [13]. Therefore no autodetachment can be observed beyond oxygen exposures of 7.5 L although the work function remains low.

The UPS results displayed in Fig. 3 show, that the intensity corresponding to emission from the underlying Mg_2Si just below E_F does not vanish for the completely oxidized surface (see top spectrum in Fig. 3). The insulating oxide layer produced during the oxidation of the Mg_2Si surface attenuates the UPS signal arising from the underlying Mg_2Si layer by an amount of ca 20%. In contrast, the MIES measurements displayed in Fig. 4 show a completely developed insulator band gap which means that no emission from states located between the valence band maximum and E_F is observed. It is therefore concluded that the oxidation produces only a thin oxide layer. Otherwise the contributions from the underlying Mg_2Si film seen with UPS should have vanished.

The top MIES spectrum of Fig. 4 for the oxidized Mg_2Si layer is compared with the MIES spectrum for an oxidized (20 L) Mg film and an oxidized Si crystal in Fig. 5a; Fig. 5b shows the corresponding UPS spectra. The Mg film was produced by evaporating Mg onto a Si(100) surface at room temperature. The Mg layer thickness amounts to 100 Å [13]. The SiO_2 surface is naturally oxidized Si(100) with an oxide thickness of 11 Å [31]. The MIES spectrum displays the pure SiO_2 valence band while UPS shows some additional contributions on the left side of the SiO_2 valence band from the underlying pure Si substrate. It is obvious that the spectra for oxidized Mg film and the oxidized Mg_2Si film in Fig. 5a (MIES) and Fig. 5b (UPS) are rather similar. In contrast, the SiO_2 surface shows a structure peaked at ca 2 eV higher binding energies. The MIES and UPS measurements suggest therefore a MgO termination of the surface. The absence of SiO_2 (Fig. 5c) contributions in the UPS spectra suggests, that there is no subsurface Si oxidation.

To improve the knowledge of the chemical composition of the oxygen induced layer, additional XPS measurements were performed. Fig. 6 shows the XPS spectra of the Mg KLL peak (Fig. 6a), the Si 2p peak (Fig. 6b) and the O 1s peak (Fig. 6c) of the Mg_2Si layer *before* and *after* oxidation with 15 L O_2, respectively. The bottom spectrum corresponds to the bottom spectra of Figs. 3 and 4; the top spectrum corresponds to the top spectra of Figs. 3 and 4.

The position of the Mg KLL peak due to Mg incorporated into the Mg_2Si is found at $E_B = 303.3$ eV, which matches the Mg KLL peak positions found for Mg layers [13] and for polycrystalline Mg samples [32]. It has been observed that the Mg 1s peak shifts by ca +0.6 eV during silicide formation [10]. The Mg 2p peak also shifts by a comparable amount during silicide formation (see Fig. 1b), so that the KLL peak, which mainly displays the energetic difference between Mg 1s and Mg 2p orbitals, remains almost unaffected. The further peaks on the right side of the bottom spectrum in Fig. 6a are also assigned to the Mg KLL peak [33]. They are in particular not caused by oxygen which is proven by the XPS

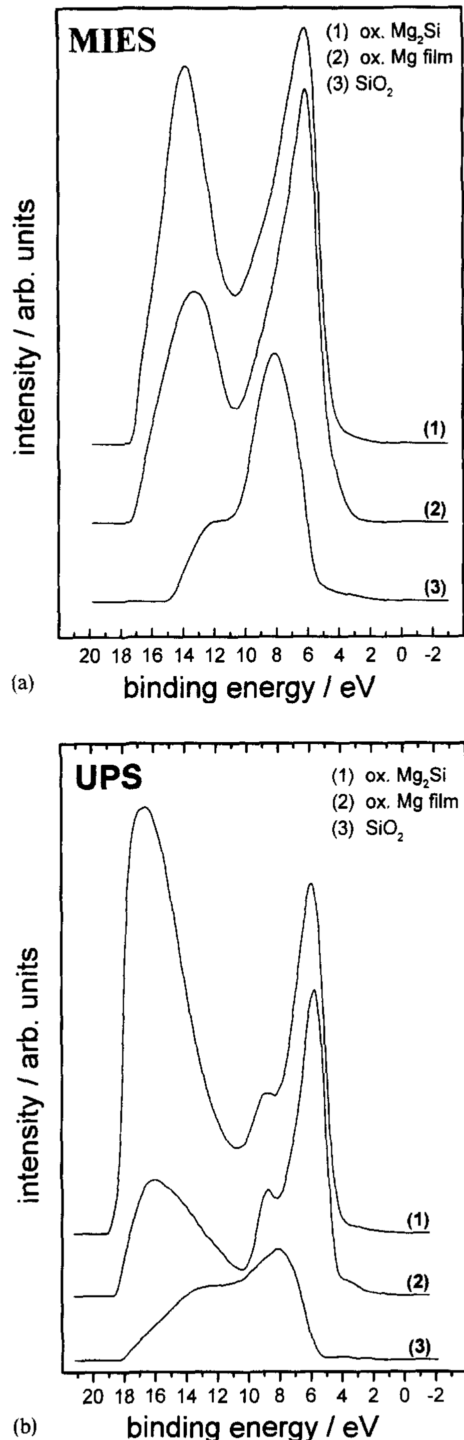

Fig. 5. (a) MIES spectra and (b) UPS spectra for an oxidized Mg film, the oxidized Mg_2Si layer and an oxidized SiO_2 surface (from Ref. [31]).

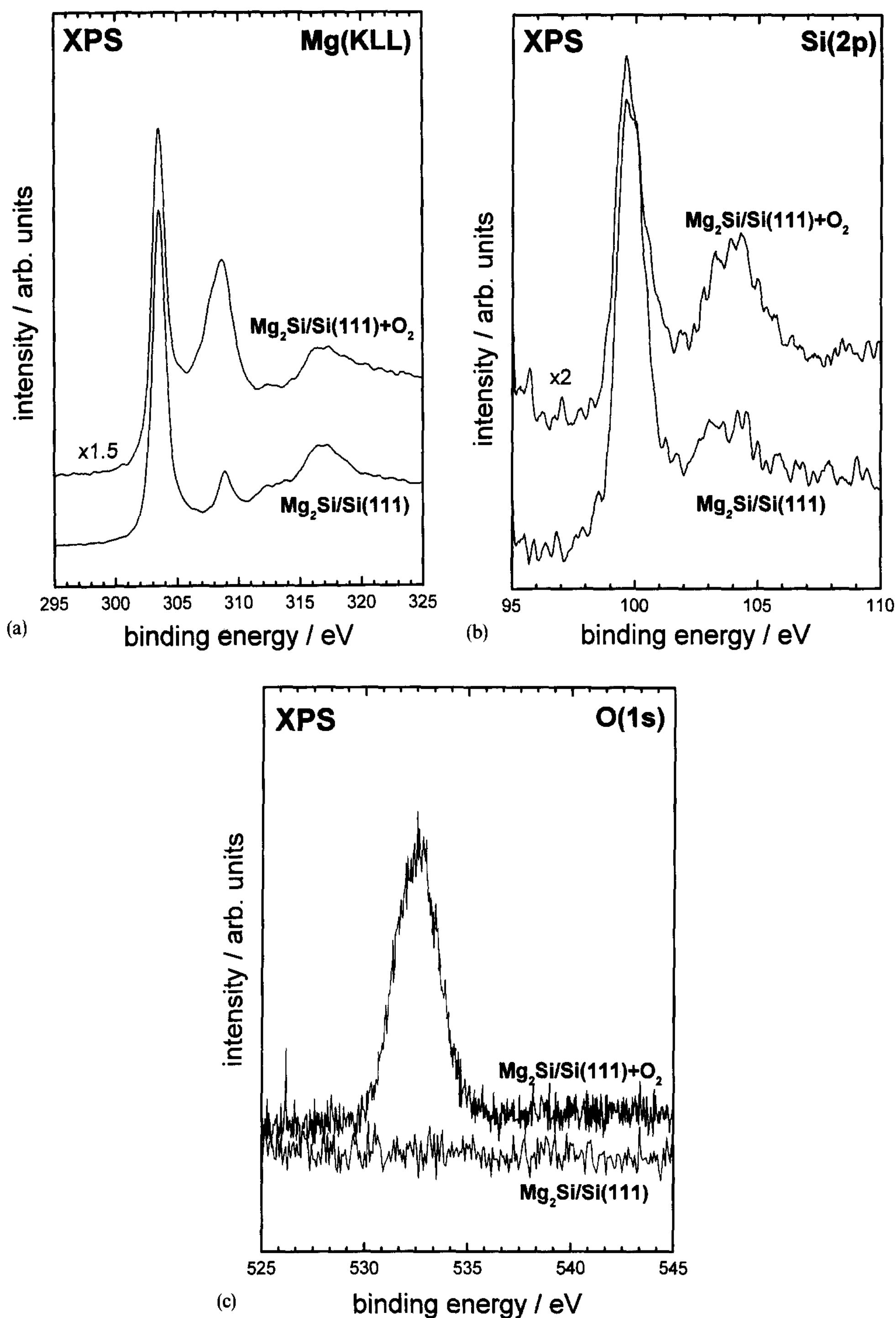

Fig. 6. XPS spectra of pure and oxidized Mg_2Si layers: (a) Mg KLL peak; (b) Si 2p peak; and (c) O 1s peak.

results for the O 1s peak of the same surfaces before and after oxidation shown in Fig. 6c.

The top spectrum in Fig. 6a shows a strong intensity increase at $E_B = 308.8$ eV caused by Mg^{2+}, which corresponds to an energetic difference to the Mg KLL peak of $\Delta E = 5.4$ eV. This is comparable to the energetic difference of $\Delta E = 5.0$ eV observed during the oxidation of Mg [13,32]. This behaviour suggests that the Mg–oxygen bonding is completely ionic like it is for oxidized Mg surfaces. A similar behaviour has been found for oxidized $TiSi_2$ surfaces [12], where TiO_2 contributions containing Ti^{4+} ions occur.

Fig. 6b shows the corresponding XPS spectra of the Si 2p peak for the clean and the oxidized Mg_2Si layer. The additional structure on the right side of the bottom spectrum for Mg_2Si is assigned to the Mg 2s emission. It is also not caused by oxygen as can be seen from Fig. 6c.

Upon oxidation the intensity at $E_B = 103.9$ eV increases by a small amount. The analysis of the peak areas of the oxygen induced peaks in Fig. 6aFig. 6b, taking into account the different excitation cross-sections, gives the relative oxide contributions of >95% of MgO and <5% of SiO_2 with an uncertainty, which amounts to 5% also. This means, that the surface is almost completely covered by MgO, which is in accordance with the results from the MIES and UPS measurements. The MIES and UPS measurements for the completely oxidized Mg_2Si surface show no contributions from SiO_2. This suggests, that the possible part of SiO_2 evaluated from the XPS measurement will be even <5%.

The almost complete absence of silicon-oxide complexes is a surprising result. For the oxidation of all other silicides published so far, a silicon oxidation takes place at least to a distinct amount, which is strongly enhanced by the metal components. Furthermore, for the most silicides metal oxidation does not take place at all or only to a small amount. For the oxidation of $TiSi_2$ the simultaneous formation of SiO_2 and TiO_2 to a comparable amount was observed [12]. The authors discussed the formation probability on the basis of the heat of formation. The heat of formation ΔH amounts to: $\Delta H(SiO_2) = -858$ kJ mol^{-1}; $\Delta H(TiO_2) = -944$ kJ mol^{-1}; $\Delta H(Mg_2Si) = -77$ kJ mol^{-1}; $\Delta H(MgO) = -601$ kJ mol^{-1} [34]. From the comparison of these values the simultaneous formation of SiO_2 and TiO_2 is not surprising, because the values are of comparable amount. In contrast, the heat of formation of PdO for example amounts to $\Delta H(PdO) = -87$ kJ mol^{-1} [34] and therefore no PdO is observed during the oxidation of Pd silicides [35]. Following this argument the formation of SiO_2 during the oxidation of the Mg_2Si surface should be more probable than for $TiSi_2$, because the heat of formation for MgO is lower than the one for TiO_2. It is very surprising, that during the oxidation of Mg_2Si no silicon-oxide is produced. The following picture is therefore suggested: the Mg_2Si surface is terminated by Mg atoms. Impinging oxygen molecules are dissociated and lead to MgO formation. After the completion of the top MgO layer further impinging oxygen molecules are no longer dissociated, thus inhibiting the subsurface oxidation. This simple model explains the results, although, at present, there is no direct proof for it.

4. Summary

Mg_2Si layers with a thickness of 100 Å are produced on Si(111) by continuous Mg evaporation at a target temperature of ca 570 K for 10 min. The layers are non-epitaxial with a surface work function of 3.3 eV. The SDOS of this layer exhibit a strong double peak just below E_F which probably arise from occupied Mg 3s orbitals. The measured chemical shifts of the core levels Si 2p and Mg 2p during silicide formation are similar to those obtained for epitaxial [5] and non-epitaxial thin Mg_2Si films [10].

The oxidation of the thick Mg_2Si layers is practically completed at exposures of ca 10 L. The surface work function decreases to 2.8 eV at this exposure. The oxidation produces a thin insulating layer formed by MgO. The electronic struture of this surface resembles closely that of MgO surfaces.

In contrast to the oxidation of all other silicides published so far, no silicon oxidation is observed. On the basis of thermodynamic arguments it is suggested, that the initial surface is terminated by

Mg atoms. After the formation of a top MgO layer further subsurface oxidation is inhibited.

References

[1] C. Calandra, O. Bisi, G. Ottaviani, Surf. Sci. Rep. 4 (1985) 271.
[2] A.H. Reader, A.H. van Ommen, P.J.W. Weijs, R.A.M. Wolters, D.J. Ostra, Rep. Prog. Phys. 56 (1992) 1397.
[3] N.E. Christensen, Phys. Rev. B 42 (1990) 7148.
[4] R.W.G.O. Wyckoff, Crystal Structures, Vol. I., Wiley, New York, 1965.
[5] C. Wigren, J.N. Andersen, R. Nyholm, U.O. Karlsson, Surf. Sci. 289 (1993) 290.
[6] J. Tejeda, M. Cardona, Phys. Rev. B 14 (1976) 2559.
[7] D. Vandré, L. Inciccia, G. Kaindl, Surf. Sci. 225 (1990) 233.
[8] J. Quinn, F. Jona, Surf. Sci. 249 (1991) L307.
[9] A.J. Bevolo, H.R. Shanks, J. Vac. Sci. Technol. A 1 (1983) 574.
[10] M.R.J. van Buuren, C.L. Griffiths, H. van Kempen, Surf. Sci. 314 (1994) 172.
[11] A. Cros, R.A. Pollak, K.N. Tu, J. Appl. Phys. 57 (1985) 2253.
[12] A. Cros, C. Pirri, J. Derrien, Surf. Sci. 152/153 (1985) 1113.
[13] D. Ochs, W. Maus-Friedrichs, M. Brause, J. Günster, V. Kempter, V. Puchin, L. Kantorovich, A. Shluger, Surf. Sci. 365 (1996) 557.
[14] G. Ertl, J. Küppers, Low Energy Electrons and Surface Chemistry. VCH Verlagsgesellschaft, Weinheim, 1985.
[15] R. Hemmen, H. Conrad, Phys. Rev. Lett. 67 (1991) 1314.
[16] W. Maus-Friedrichs, M. Wehrhahn, S. Dieckhoff, V. Kempter, Surf. Sci. 237 (1990) 257.
[17] W. Maus-Friedrichs, S. Dieckhoff, V. Kempter, Surf. Sci. 249 (1991) 149.
[18] J. Lee, C. Hanrahan, J. Arias, F. Bozso, R.M. Martin, H. Metiu, Phys. Rev. Lett. 54 (1985) 1440.
[19] B. Woratschek, W. Sesselmann, J. Küppers, G. Ertl, H. Haberland, Phys. Rev. Lett. 55 (1985) 611.
[20] A.G. Borisov, D. Teillet-Billy, J.P. Gauyacq, Surf. Sci. 284 (1993) 337.
[21] J. Günster, Th. Mayer, V. Kempter, Surf. Sci. 359 (1996) 155.
[22] S. Schippers, S. Oelschig, W. Heiland, L. Folkerts, R. Morgenstern, P. Eeken, I.F. Urazgil'din, A. Niehaus, Surf. Sci. 257 (1991) 289.
[23] P. Eeken, J.M. Fluid, A. Niehaus, I.F. Urazgil'din, Surf. Sci. 273 (1992) 160.
[24] J. Günster, Th. Mayer, M. Brause, W. Maus-Friedrichs, H.G. Busmann, V. Kempter, Surf. Sci. 336 (1995) 341.
[25] F. Wiegershaus, S. Krischok, D. Ochs, W. Maus-Friedrichs, V. Kempter, Surf. Sci. 345 (1996) 91.
[26] W.C. Price, in: C.R. Brundle, A.D. Baker (Eds.), Electron Spectroscopy: Theory, Techniques and Applications, Vol. I. Academic Press, London, 1977, p. 151.
[27] W. Maus-Friedrichs, S. Dieckhoff, M. Wehrhahn, S. Pülm, V. Kempter, Surf. Sci. 271 (1992) 113.
[28] W. Maus-Friedrichs, S. Dieckhoff, V. Kempter, Surf. Sci. 273 (1992) 311.
[29] M. Cardona, J. Tejeda, N.J. Shevchik, D.W. Langer, Phys. Stat. Solid (b) 58 (1973) 483.
[30] D. Ochs, M. Brause, B. Braun, W. Maus-Friedrichs, V. Kempter, Proceedings of ECASIA, Sweden, 1997.
[31] Th. Mayer, Diploma Thesis TU Clausthal, 1995, unpublished data.
[32] J.C. Fuggle, Surf. Sci. 69 (1977) 581.
[33] C.D. Wagner, W.M. Riggs, L.E. Davis, J.F. Moulder, G.E. Muilenberg, Handbook of X-ray Photoelectron Spectroscopy, Perkin Elmer, New York, 1979.
[34] Landolt-Börnstein, Zahlenwerte und Funktionen, 6 Edn. Springer Verlag, Berlin, 1961.
[35] A. Cros, R.A. Pollak, K.N. Tu, Thin Solid Films 104 (1983) 221.